MaLoc: A Practical Magnetic Fingerprinting Approach to Indoor Localization using Smartphones

Hongwei Xie, Tao Gu†, Xianping Tao, Haibo Ye, Jian Lv
State Key Laboratory for Novel Software Technology, Nanjing University, Nanjing, China
†RMIT University, Melbourne, Australia
{hongwei.xie.90, yehb.ye}@gmail.com, tao.gu@rmit.edu.au, {txp,lj}@nju.edu.cn

ABSTRACT

Using magnetic field data as fingerprints for localization in indoor environment has become popular in recent years. Particle filter is often used to improve accuracy. However, most of existing particle filter based approaches either are heavily affected by motion estimation errors, which makes the system unreliable, or impose strong restrictions on smartphone such as fixed phone orientation, which is not practical for real-life use. In this paper, we present an indoor localization system named MaLoc, built on our proposed augmented particle filter. We create several innovations on the motion model, the measurement model and the resampling model to enhance the traditional particle filter. To minimize errors in motion estimation and improve the robustness of particle filter, we augment the particle filter with a dynamic step length estimation algorithm and a heuristic particle resampling algorithm. We use a hybrid measurement model which combines a new magnetic fingerprinting model and the existing magnitude fingerprinting model to improve the system performance and avoid calibrating different smartphone magnetometers. In addition, we present a novel localization quality estimation method and a localization failure detection method to address the "Kidnapped Robot Problem" and improve the overall usability. Our experimental studies show that MaLoc achieves a localization accuracy of 1∼2.8m on average in a large building.

ACM Classification Keywords

C.2.m Computer Systems Organization: COMPUTER-COMMUNICATION NETWORKS—*Miscellaneous*

General Terms

Algorithms, Experimentation, Performance

Author Keywords

Indoor Localization, Magnetic, Particle Filter, Smartphone

INTRODUCTION

Indoor localization using smartphones has attracted much interests in recent years due to an increasing number of location-based applications that require accurate positioning or continuous tracking in buildings. The Wi-Fi fingerprinting based approach looks promising as it leverages on the widely available Wi-Fi infrastructure. This approach does not require any specialized hardware or additional infrastructure support. However, tracking the location of a mobile user requires frequent Wi-Fi scanning which is quite power hungry. In addition, the effectiveness of Wi-Fi fingerprinting depends on a number of factors including the number of Wi-Fi access points deployed, spatial differentiability, and temporal stability of the radio environment [20].

With the availability of embedded sensors on smartphones, a new fingerprinting approach based on magnetometer has been proposed [11, 12, 22]. This approach is based on the hypothesis that in an indoor setting the magnetic field is highly non-uniform, and the magnetic field fluctuations arise from both natural and man-made sources (e.g., steel and concrete structures and electric systems). The abnormalities of the magnetic field can be used as fingerprints for indoor localization. While this approach shares a similar idea as Wi-Fi fingerprinting, it certainly has several advantages [2, 7, 13, 22]: 1) independent from the Wi-Fi infrastructure; 2) more reliable than Wi-Fi; 3) the change of magnetic field with location is quite significant, allowing for precise positioning; 4) more power efficient.

Different from Wi-Fi fingerprints which combine the radio signal strength from multiple access points, a magnetic fingerprint is basically a 3-axis vector which consists of the magnetic field readings along the phone's three axes (X, Y and Z). Studies [2, 7, 21] show that in a large indoor space the magnetic fingerprints may not be unique. As a result, large localization error may occur. Most of the existing work [4, 11, 12] leverage on Particle Filter (i.e., Monte Carlo Localization or MCL) to solve this problem and improve accuracy. The basic principle is to use random samples (also referred to as particles, i.e., hypothesis for the user's state such as position and heading direction) to represent the posterior distribution of the user's state. Particle filter recursively re-samples a set of particles according to a series of magnetic fingerprints and their spatial correlations to converge to the poster distribution of true state. The spatial correlations can be obtained through user motion estimation. Therefore, the performance of particle filter depends on: 1) motion estimation; 2) fingerprint measurement and the magnetic fingerprinting model; and 3) resampling.

UbiComp'14, September 13 - 17, 2014, Seattle, WA, USA

http://dx.doi.org/10.1145/2632048.2632057

Existing particle filter based approaches have several limitations. First, magnetometer readings are associated with phone orientation. When the phone changes its orientation, we get different vectors. One may collect and store the magnetic readings of all directions at any location [4, 7], which incurs high training cost, or use coordinate transformation [12], which is error-prone. But both measurement models result in the work based on particle filter [4, 11, 12] typically require the smartphone to head the same way as the user. This is obviously not practical. Moreover, the magnetometers on different smartphones have to be carefully calibrated before use. Magnetometer calibration is difficult considering a large number of smartphones. Therefore, a better measurement model and a magnetic fingerprinting model are needed.

Second, existing motion estimation methods are error-prone. Particle filter is mostly used for tracking mobile robots [9, 25]. When applied to smartphone tracking, the motion estimation usually incurs much more noise than robots, such as step miscounting, step length estimation error, or change of heading offset (i.e., the difference between user heading and phone heading). These errors easily lead to localization failure.

Third, existing particle filter methods suffer from the well-known "Kidnapped Robot Problem" [24], in which the robot may believe it knows where it is while it does not. This may turn into a serious problem when localizing smartphones, i.e., it may take a long time for the particle filter to realize localization failure, where localization errors can be arbitrary in this period. Hence, a fast failure detection mechanism during runtime is highly desired.

In this paper, we present a systematic approach to the design of a practical and precise localization system, named MaLoc (**Ma**gnetic fingerprinting based indoor **Loc**alization). We propose an augmented particle filter, aiming to address the aforementioned issues. Firstly, we propose a hybrid measurement model to improve system performance. It combines a novel magnetic fingerprinting model with the common magnetic density fingerprinting model. The novel magnetic fingerprint model is obtained by extracting both the horizontal and vertical components of the magnetic vector, which has the key features of being independent from phone orientation. We also explore the gradient of magnetic fingerprints to avoid calibrating different smartphone magnetometers. Secondly, we propose a novel motion estimation method covering step counting, step length estimation and user heading change estimation, which is independent from phone orientation. To minimize estimation errors and improve system robustness, we propose a dynamic step length estimation algorithm and a heuristic resampling algorithm. Specially, the heuristic resampling algorithm allows smartphone for other use such as answering a call while walking, whereas in traditional particle filter it may arise heading offset change and introduce large errors into heading change estimation, and hence result in localization failure. Thirdly, we propose a localization quality estimation method by utilizing the clustering degree of particles. Based on this method, we design a localization failure detection method to address global localization failure, and our experiments show it is able to detect 92.6% of localization failure. Finally, we develop an efficient crowdsourcing method to collect magnetic fingerprints, aiming to improve the existing time-consuming and labor-intensive collection process [13].

With the proposed models and methods, MaLoc has practical implications with no restriction on smartphone's orientation, and being able to run in background without intervening other phone applications. In summary, this paper makes the following contributions.

(1) We propose an augmented particle filter to improve the system performance and robustness, which includes a dynamic step length estimation method to compensate the uncertainty of user's true step length, a heuristic particle resampling mechanism to solve the heading offset change problem, and a novel localization quality estimation and localization failure detection method.

(2) We propose a novel hybrid measurement model, which is independent from phone orientation, to improve system performance. Moreover, it avoids calibrating different smartphone magnetometers.

(3) MaLoc has no restrictions on phone orientation and usage, which has significant implications for real applications. We conduct comprehensive experiments, and the results show that MaLoc achieves an accuracy of 1$\sim$2.8 meters in a large building, and it is more power-efficient than Wi-Fi scanning.

The paper is organized as follows. Section 2 describes the related work. Section 3 reviews the background and our empirical studies of magnetometer and magnetic filed. Section 4 presents the architecture of MaLoc. The motion model and the magnetic measurement model are introduced in Sections 5 and 6, respectively. Section 7 presents the localization quality estimation and the localization failure detection algorithm. Section 8 describes the method for building the fingerprint database. Section 9 describes the experiments, and finally Section 10 concludes the paper.

RELATED WORK

Much work has been done in indoor localization over the past decade. Many systems are built upon special infrastructures such as infrared [28], acoustic [29] and bluetooth [10]. It is usually very costly deploying these infrastructures. Other systems leverage on existing, widely available infrastructures, such as GSM, Wi-Fi, and FM. Earlier Wi-Fi based approaches use a propagation model of receiving signal strength (RSS) from Wi-Fi access points (APs) to compute the receiver's location [15]. However, building such a model often requires the prior knowledge of AP positions and the accuracy much depends on the multi-path fading effect. EZ [6] does not require any explicit pre-deployment effort of Wi-Fi APs, but it comes at the cost of loss of accuracy, in which the median localization error may be up to 7m in a large building environment. The Wi-Fi fingerprinting based approach becomes popular in recent years as it does not require any prior knowledge about APs, as well as it does not leverage on the

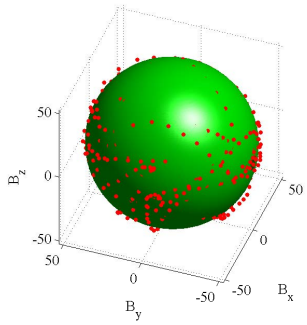

Figure 1. Locus of magnetic readings with the optimum ellipsoidal fit superimposed.

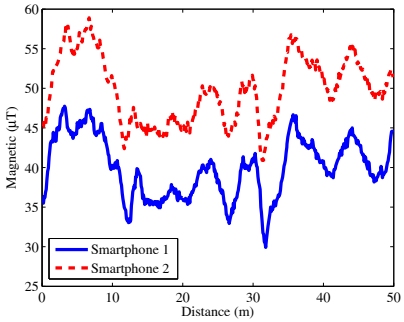

Figure 2. Magnetic readings captured by two smartphones along a 50-meter corridor.

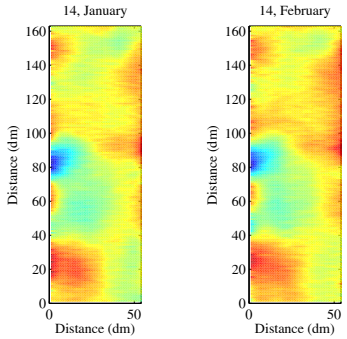

Figure 3. Magnetic field map captured by smartphones over one month.

propagation model. Using Wi-Fi fingerprinting, RADAR [3] and Horus [31] achieve 3-5m and 2m localization accuracy, respectively. However, the Wi-Fi RSS is sensitive to human presence, and it may vary from time to time, limiting localization accuracy. PinLoc [20] improves the accuracy within 1m by leveraging the physical layer but extensive profiling is required. FM fingerprinting is also feasible for indoor localization. Chen et al. [5] used FM signals which is more energy efficient than Wi-Fi fingerprinting, but localization can only be done in room level. GSM based indoor localization methods [27] have also been proposed to work with a coarse precision.

Recently years, magnetic field has been explored as fingerprints for robot localization [23]. Haverinen et al. [11] proposed an indoor localization system using particle filter for both pedestrian and robot in the corridor of a building. Their system requires the user's heading must keep consistent with the corridor while walking. Chung et al. [7] proposed a system which requires to measure the magnetic readings of all directions at any position and localization is done with an array of magnetometers. Their system achieves an accuracy of 4.7 meters, however, the training cost is quite high. Some work has been proposed using magnetometer on smartphones. LocateMe [22] investigated a magnetic model using smartphones, and localization can be achieved in room level. However, it is restricted in a 1-D environment, such as corridor. Bilke [4] proposed a localization system which works in an 2-D environment with the mean localization error of 4 meters; but its training cost is comparable to the work done in [7]. The system proposed in [12] also works in 2-D environment and is able to avoid the measurements for all directions by coordinate transformation. However, it is error-prone because orientation estimation contains errors which will be amplified by matrix transformation. No evidence in that paper was found that the system works in practise. The systems proposed in [4, 11, 12] are all based on particle filter, however they typically require the smartphone's heading to be the same as the user all the time. The main problem of using inertial sensors (pedestrian dead-reckoning) for localization [14, 30] is that small errors in sensing may be magnified by integration [19]. By introducing particle filter or other methods (i.e., kalman filter) for sensor fusion, the errors in measuring inertial sensors can be filtered out or minimized.

While we leverage on particle filter in this work, we have no restriction on phone orientation during localization. Mobile users are able to use their smartphones as usual. To achieve this, we propose an augmented particle filter which requires the motion estimation and the magnetic fingerprinting models must be independent from phone orientation. To this extent, MaLoc is more practical than existing magnetometer based localization systems.

MAGNETIC FIELD AND MAGNETOMETER

In this section, we review the background of the geomagnetic field and magnetometer on smartphones, and conduct preliminary empirical studies.

Characteristics of Magnetometer on Smartphone

The magnetic field value $\boldsymbol{B}_p$ is measured by a smartphone's magnetometer. $\boldsymbol{B}_e$ is the magnetic field vector at the same location in earth coordinate system, which is combined with the geomagnetic field and the magnetic field from the environment. $\boldsymbol{B}_p$ is obtained by the phone rotated in yaw ψ, pitch θ and roll ϕ from $\boldsymbol{B}_e$, respectively. Its relationship with $\boldsymbol{B}_e$ is defined as Equation(1) in absence of noise [18].

$$\boldsymbol{B}_p = \boldsymbol{R}_x(\phi)\boldsymbol{R}_y(\theta)\boldsymbol{R}_z(\psi)\boldsymbol{B}_e \quad (1)$$

$$\boldsymbol{B}_e = \boldsymbol{B}_{geomagnetic} + \boldsymbol{B}_{environment} \quad (2)$$

where $\boldsymbol{R}_z(\psi)$, $\boldsymbol{R}_y(\theta)$, $\boldsymbol{R}_x(\phi)$ are the corresponding rotation matrices. When we include the noise: hard-iron effect $\boldsymbol{V}$ and soft-iron effect $\boldsymbol{W}$, $\boldsymbol{B}_p$ is defined as Equation(3) [18].

$$\boldsymbol{B}_p = \boldsymbol{W}\boldsymbol{R}_x(\phi)\boldsymbol{R}_y(\theta)\boldsymbol{R}_z(\psi)\boldsymbol{B}_e + \boldsymbol{V} \quad (3)$$

The hard-iron effect $\boldsymbol{V}$ is an offset vector and the soft-iron effect $\boldsymbol{W}$ is a matrix. Because of noise, when the smartphone is rotated at a fixed point, the locus of the magnetic reading will be an ellipsoid, as shown in Fig. 1. After calibrating these noise, the locus will be closed to the sphere.

Different smartphones may have different types of magnetometers that vary in their sensitivities. Even the same type of smartphone may read different magnetic values at the same location. Figure 2 shows the magnetic readings captured by two Galaxy Nexus smartphones along a 50-meter long corridor. Their readings fluctuate at the same location, but the gradients of these two curves remain quite constant. This suggests that we can use the gradients of fingerprints instead of

raw fingerprint values to avoid calibrating different magnetometers.

Characteristics of Magnetic Field

The indoor magnetic field combines the geomagnetic field and the fields from ferromagnetic objects. We are interested to study the factors which may have influence on the magnetic field readings. Figure 3 shows the magnetic density map captured by a smartphone in a 16.3m×5.4m indoor area over one month. As we can see, magnetic field readings are quite stable over time, but changed significantly with locations. We also study the magnetic field readings when a smartphone is placed in different height, as shown in Fig. 4. The magnetic readings are collected in a height of 0.5m, 1m and 1.5m from the floor, respectively, along a corridor. Considering errors in the location mapping, the differences are not as significant as the horizontal differences, and their gradients are still very similar. In addition, previous studies [2, 7, 13, 22] also demonstrate that the effects caused by objects carried by the user, other pedestrians and the rearrangement of furniture are very limited. From these studies, we confirm the feasibility of using magnetometer on smartphone for indoor localization.

MALOC ARCHITECTURE

We now describe how MaLoc works. MaLoc is built on an augmented particle filter. The particle filter use a set of particles to estimates the posterior distribution of a system-state conditioned on measurements. The system-state or user-state here is the user's position and heading:

$$\boldsymbol{s} = (x, y, \theta) \tag{4}$$

where x, y represents the user's position and θ is the user's heading direction. A particle is a hypothesis for the user's state with a weight:

$$\chi_i =< \boldsymbol{s}_i, w_i > \tag{5}$$

where w_i is the weight of the particle. A higher weight means it more close to the true state, and the posterior distribution of user's state can be represented by a set of particles.

The particle filter contains three essential components: the motion model, the measurement model and the resampling model, as presented in Algorithm 1. The motion model updates each particle's state by estimating user's motion leveraged on the inertial sensors. The measurement model then re-evaluates the particles' weights. Finally, the remaining particles refined by resampling will be more close to the true system state. As a rule, with the recursive operations of the three processes, the prediction for true state will become more and more accurate. Essentially, the performance of a particle filter based method completely depends on how these three models construct.

In MaLoc, N particles are randomly sampled from the initial area given by a coarse-grained localization method. The loop is controlled by step counting. For each step a user moves, we will update the particles and prediction.

Algorithm 1 Procedure of MaLoc

```
Generate N random particles from an initial area.
for each step do
    Estimate l and Δθ.
    for each particle do
        Update position and heading by motion model as Equation (6) and (7).
        Evaluate the weight of particles by measurement model as Equation (9).
    end for
    Decide the amount of particles for each resampling method N_d and N_h. (N = N_d + N_h)
    Resample N_d particles from old particles according to the distribution of their weights.
    Resample N_h particles by our heuristic method.
    Normalize the weights.
    Predict the user's state by Equation (10).
    Estimate the quality of localization.
    if detect localization failed then
        Run recover procedure.
    end if
end for
```

We construct the motion model as Equation(6) and (7):

$$\theta_i^{t+1} = \theta_i^t + \Delta\theta + G_\theta \tag{6}$$

$$\begin{bmatrix} x_i^{t+1} \\ y_i^{t+1} \end{bmatrix} = \begin{bmatrix} x_i^t \\ y_i^t \end{bmatrix} + \begin{bmatrix} cos(\theta_i^{t+1}) \\ sin(\theta_i^{t+1}) \end{bmatrix} \times (l + G_l) \tag{7}$$

where l is the step length, $\Delta\theta$ is the user's heading changes between two consecutive steps, G_l and G_θ are Gaussian noise. Different from existing work [4, 8, 11, 12], the step length l is not constant in MaLoc, and it is estimated dynamically during localization. The step length is different from one user to another, and even one person's step length may be changed. Inaccurate step length estimation will lead to large localization errors, resulting in localization failure, which has been shown in the experiment in Section 9. We propose a dynamic step length estimation algorithm to effectively solve these uncertainties. The algorithm also makes MaLoc error tolerant in step counting. $\Delta\theta$ is obtained from the gyroscope sensor on smartphones with transformation. Generally, $G_l \sim N(0, \sigma_l)$ and $G_\theta \sim N(0, \sigma_\theta)$ are used to enlarge the diversity of particles.

We use magnetic fingerprints as the main observation values $\boldsymbol{z}$ in the measurement model. $P(\boldsymbol{z}|\boldsymbol{s})$ is the probability of observing $\boldsymbol{z}$ on state $\boldsymbol{s}$, which depends on the intensity of changes of magnetic field at that location and on the age of the map. Since it is difficult to obtain $P(\boldsymbol{z}|\boldsymbol{s})$, the Gaussian pseudo-distribution [4, 11, 12] are often used, as presented in Equation(8).

$$P(\boldsymbol{z}|\boldsymbol{s}) = \frac{1}{(2\pi)^{n/2}|\boldsymbol{V}|^{1/2}} exp\{-\frac{1}{2}[\boldsymbol{z} - obv(\boldsymbol{s})]^T \boldsymbol{V}^{-1}[\boldsymbol{z} - obv(\boldsymbol{s})]\} \tag{8}$$

where n is the dimension of $\boldsymbol{z}$, $\boldsymbol{V}$ is the covariance, $obv(\boldsymbol{s})$ is a function to get the observation value of state $\boldsymbol{s}$ in the

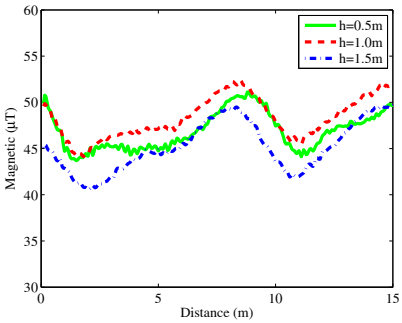

Figure 4. Magnetic readings captured by smartphone with different heights.

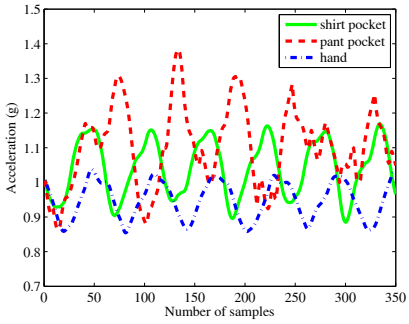

Figure 5. The magnitude of acceleration readings captured by a smartphone carried in different positions.

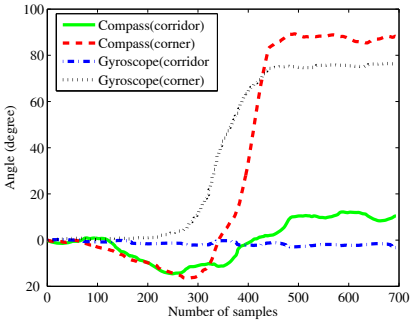

Figure 6. The angle changes captured by compass and gyroscope when walking along a corridor and turning at a 90-degree corner.

fingerprint database. A hierarchical data structure has been designed for fast obtaining the observation value. We evaluate each particle by Equation(9) instead of using a Bayes filter model $w_i^{t+1} = w_i^t P(\boldsymbol{z^{t+1}}|\boldsymbol{s_i^{t+1}})$ or directly use $w_i^{t+1} = P(\boldsymbol{z^{t+1}}|\boldsymbol{s_i^{t+1}})$ like others. In this way, MaLoc is more stable, and importantly it avoids calibrating different magnetometers.

$$\begin{aligned} w_i^{t+1} &= P(\boldsymbol{z^{t+1}} - \boldsymbol{z^t}|\boldsymbol{s_i^t}, \boldsymbol{s_i^{t+1}}) \\ &= \frac{1}{(2\pi)^{n/2}|\boldsymbol{V}|^{1/2}} exp\{-\frac{1}{2}[(\boldsymbol{z^{t+1}} - \boldsymbol{z^t}) \\ &- (obv(\boldsymbol{s_i^{t+1}}) - obv(\boldsymbol{s_i^t}))]^T \boldsymbol{V}^{-1}[(\boldsymbol{z^{t+1}} - \boldsymbol{z^t}) \\ &- (obv(\boldsymbol{s_i^{t+1}}) - obv(\boldsymbol{s_i^t}))]\} \end{aligned} \tag{9}$$

Resampling is to get rid of the particles with low weights which contribute almost nothing to the prediction, and focus resources on particles which are close to the true state with higher probability. In this work, we resample new particles from old ones according to the discrete probability distribution generated by their weights (i.e., a traditional resampling method). However, it may result in loss of particle diversity and localization failure when large noise (e.g., the change of heading offset) is introduced. To address this, we propose a heuristic resampling method to work together with the traditional resampling method. Finally, we estimate the true state with the weighted average of the current particles, as shown in Equation (10).

$$\hat{\boldsymbol{s}} = \sum_{i=1}^{N} \boldsymbol{s_i} \cdot w_i \tag{10}$$

where the weight w_i has been normalized.

As we can see, the current particles are generated from the last round of localization. That is, if an error occurs in most of the particles close to the true state wiped out, it may end up with wrong prediction in the following rounds of localization. To better address this issue, we propose a localization quality estimation approach to estimate the precision of current localization and detect if the localization fails. In the case of localization failure, MaLoc runs a recover procedure to guarantee the usability of the system.

MOTION MODEL

In this section, we introduce the methods for step counting, dynamic step length estimation, and heading change estimation. We also present the heuristic resampling algorithm along with heading changes estimation. The proposed augmented particle filter with dynamic step estimation and heuristic resmapling will enhance the robustness of the existing particle filter.

Steps Counting

We use accelerometer on smartphone for step counting. Since smartphone may be carried by a user in any orientation, we only extract the magnitude of the accelerometer reading. The mean filter is used to smooth the raw acceleration data. As shown in Fig. 5, the acceleration values are captured by a smartphone carried in different ways, e.g., in hand, in the shirt pocket, and in the front pant pocket. The result shows that counting the number of peaks or valleys may not work for all cases. There are also many step counting algorithms in the literature [19, 16], which achieved hight accuracy. In this work, we use a simple one for lower computation overhead. We set four thresholds, T_{acc}^u, T_{acc}^d and T_{time}^u, T_{time}^d, to filter false cases. T_{acc}^u and T_{acc}^d are the upper bound and lower bound of the acceleration variance between two adjacent peak and valley. T_{time}^u and T_{time}^d are the upper bound and lower bound of the time interval between them. In this way, step counting achieves better accuracy.

Dynamic Step Length Estimation

Simply, one can set a constant step length for each user. However, this is not practical as people's step lengths may vary widely. Even the step length of the same user may be changed from time to time. Since the precision of estimating a user's step length has a large impact on localization accuracy, we propose a dynamic step length estimation algorithm. It is based on this idea that when the particles are updated by the motion model, every particles evolve with different step lengths. The distribution of all particle's step lengths is $D_l \sim N(l, \sigma_l)$. Therefore, the average $l_{ave} = \frac{1}{N}\sum_{i=1}^{N} l_i$ will be very close to l. However, after resampling, all the particles will be re-evaluated and refined. A particle with a higher weight is more close to the true state. On the other hand, this particle's step length is also closer to the true step length.

The weighted average step length after resampling is defined as Equation(11).

$$l_{weighted} = \sum_{i=1}^{N_d} l_i \cdot w_i \tag{11}$$

where N_d is the number of particles sampled from old particles (See Algorithm 1), because only these parts of particles evolve from the old particles by taking a step. We then conclude that if the particle filter converges in the right way, $l_{weighted}$ will tend to be the true step length. Certainly, if the particle filter cannot converge correctly, this theory may not be guaranteed. Based on this theory, we design a dynamic step length estimation algorithm. Instead of just using $l_{weighted}$ as step length, we design a queue Q size of Q_{size} to cache the most recent l_{weight}. Their average value is used as the estimation of step length for the next round of localization. In this way, we can prevent the accidental bad converge result from influencing the estimation. Considering when the user's heading changes, his step length may have some changes, resulting in uncertain influence on the step length estimation. In our algorithm, we will not put this part into the queue. Compared with the step length estimation methods in [14, 19] who update step length model only at the turning, our algorithm can update step length in real time and does not depend on the accuracy of turn detection.

Heading Change Estimation and Change of Heading Offset

Determining the heading of a user is difficult even the compass sensor is precise in indoor environments since the user's heading may be different from phone heading (a.k.a. heading offset). In this work, we assume the initial orientation of the user is unknown which may not be the same with the phone, and eventually we use the augmented particle filter to obtain the user's heading. The heading change between two consecutive steps $\Delta\theta$ is required by the motion model. It is reasonable that we assume the phone heading is relatively stable with the user when walking. Certainly, the assumption can't hold all the time as the user may use the mobile phone for other tasks during localization, such as receiving a phone call and sending a message. These interference motions may change the heading offset and bring errors into heading change estimation. Therefore, there are two issues here: (1) how to estimate the phone's heading change between two consecutive steps regardless of its orientation and position; (2) how to eliminate the error introduced by the change of heading offset.

Compass and gyroscope on smartphone can be used for estimating the phone's heading change between two adjacent steps. Since compass does not work well in indoor environments, gyroscope may be a better choice. The gyroscope on a smartphone measures the angular velocity around the phone's x, y and z axis, respectively. Usually, the output of gyroscope is integrated over time to calculate a phone's rotation which describes the angle change. However, we cannot get the heading changes directly as the phone's orientation is unknown. We make use of the gravity sensor on smartphone to obtain the angle changes around the gravity direction, which is the same as the heading change. Figure 6 compares the performance of heading change estimation using compass and gyroscope. It depicts the angle changes with the start point when walking along a corridor and a 90-degree corner. As we can see from the figure, the measurements of gyroscope is more stable than that of compass. The large error of compass at some positions may lead to localization failure. The error of gyroscope may contribute to integration and the errors from the gravity sensor. Although the overall error may accumulate, it is quite small within one step that can be tolerated by the particle filter as each particle randomly adds a Gaussian noise in the motion model.

The change of heading offset has certainly negative impact on traditional particle filter based methods. For example, in the case that the user answers a phone call while walking, the user's heading keeps the same but the phone's heading may be changed 180 degrees. As a result, all particles reverse their headings and lost in the trap. The localization error will become bigger and bigger, and eventually result in localization failure. Therefore, detecting large heading change of the phone is risky, it may be done by the user's turning or the change of heading offset. We propose a heuristic algorithm to solve this problem, inspired by the random particle filter [24] which randomly samples new particles when the total non-normalized weight decreases. Our algorithm heuristically samples parts of new particles in the resampling phase instead of only sampling from the old particles (See Algorithm 1). How to generate new particles and how many particles are related to the phone's heading changes of this step. We have the following rules.

(1) The number of new particles N_h is proportional to $\Delta\theta$. To implement it in MaLoc, we present Equation(12).

$$N_h = \frac{\Delta\theta \cdot p}{\pi} N, N_h \leq N \tag{12}$$

where p is the parameter to control the sensitivity (usually chosen from $[0.5, 0.85]$ in our experiments), and N is the total number of particles.

(2) The position of new particles are randomly sampled from the r-meter range of the previous predicted location $(\hat{x}, \hat{y})$. r can be a constant value or a variable related to $\Delta\theta$. For simplicity, we set it as a constant value in our experiments.

(3) The initial heading of new particles are also randomly sampled from the range $[\hat{\theta}, \hat{\theta} + 2\Delta\theta]$ or $[\hat{\theta} + 2\Delta\theta, \hat{\theta}]$. $\hat{\theta}$ is the previous predicted heading.

The heuristic resampling algorithm can also increase the diversity of particles, which will make the particle filter more robust and tolerate more motion estimation errors, with the cost of decreasing the localization precision.

MAGNETIC MEASUREMENT MODEL

The magnetic measurement model evaluates particles based on the magnetic field observations captured from smartphones. As mentioned before, a magnetometer reading consists of a three-dimensional vector $\boldsymbol{B}_p = (B_x, B_y, B_z)$, representing the magnetic value along the phone's x, y, and z

axis, respectively. Generally, there are three ways of using $\boldsymbol{B}_p$ as observation values.

Using $\boldsymbol{B}_p$ directly as observation $\boldsymbol{z}$ [4, 7, 11, 12]. One method is to collect the magnetic field readings of all directions at any location, which not only increases the training cost rapidly, but also reduces the accuracy as the sample space becomes larger. Alternatively, we can estimate phone orientation and transform $\boldsymbol{B}_p$ to the earth coordinate system $\boldsymbol{B}_e$. However, this is error-prone because orientation estimation usually contains errors and these errors will be amplified on $\boldsymbol{B}_e$. Both of these two methods have a serious problem that they require the phone's heading to be the same as the user's heading during localization. Because in the measurement phase, each particle obtains the reference fingerprint $\boldsymbol{B}_{x,y,\theta}$ at a location from the database according to its position (x, y) and heading θ (not phone's heading θ_p due to inaccurate compass readings). As θ represents user's heading, if it is not the same as the phone's heading θ_p, the magnetic field reading on smartphone cannot map with any particle's observation $\boldsymbol{B}_{x,y,\theta}$ as it should be mapped to $\boldsymbol{B}_{x,y,\theta_p}$. This may result in localization failure. Therefore, using this type of observation on smartphone is not practical.

Using the magnitude B of $\boldsymbol{B}_p$ as observation [11, 22]. B is a rotation invariant scalar quantity and quite stable. However, the elements in each fingerprint will drop from three to one, reducing the uniqueness of each fingerprint. In large indoor environments, the particle filter may need more time to converge to the right location.

Extracting the horizontal component B_h and vertical component B_v of $\boldsymbol{B}_p$ as observation [13]. The gravity sensor on smartphone provides us the direction of gravity (i.e., the vertical direction). We can extract both the vertical and horizontal components of $\boldsymbol{B}_p$ and construct a new observation value (B_h, B_v) (named HV fingerprint). Figure 7 shows the magnetic field map of these two components in an indoor area. Obviously, it is more unique than the magnitude fingerprint, which will make the particle filter converge to the right location faster. This fingerprint model was mentioned in Ref [13], but there is no real-world magnetic fingerprinting based indoor localization system depends on it. That is because the gravity sensor reading is very precise when the user stands still. However, noise will be introduced when the user moves, resulting in decreasing in precision or even localization failure.

In this work, we combine both the magnitude B and (B_h, B_v) using a hybrid measurement model. The HV fingerprint has the advantage of more uniqueness, and it makes the particle filter converge to the right location faster. However, it is not as stable as the magnetic magnitude fingerprint. Therefore, we use the HV fingerprint to accelerate the convergence of MaLoc when localization starts, and then we switch it to the magnetic magnitude fingerprint for "tracking".

Since calibrating the offset of different phones' magnetometers is very costly, we just use the variance of the fingerprint value between two consecutive steps (the gradient) instead of using the fingerprint itself to avoid calibrating different magnetometers. As we mentioned before, it is also less sensitive with the changes of magnetic field in the vertical direction and the changes along with time. This is one of the reasons that we use Equation(9) to evaluate the particles. Another one is that although using the Bayes filter model to evaluate the particles will make particle filter converge more quickly and good for exposing localization failure, it also makes the particle filter become very sensitive to noise and may fail easily.

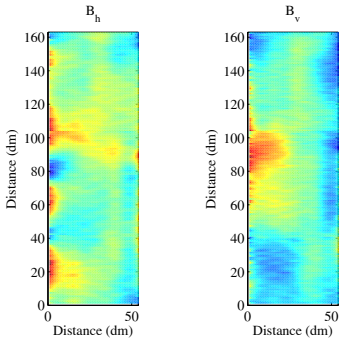

Figure 7. Magnetic field map of the horizontal component (left) and vertical component (right) in a 16.3m x 5.4m indoor area.

In a very large indoor environment, these fingerprint models or measurement models may not be suitable for localization because the particle filter will need too many particles and a long period of time to converge, incurring high computational overhead and reducing the usability. To address this issue, we leverage on a simply coarse-grained localization method [7, 12] (with 15m$\sim$30m or room level accuracy) which narrows the searching space in the initial phase only.

LOCALIZATION QUALITY ESTIMATION AND LOCALIZATION FAILURE DETECTION

For particle filter based methods, failure detection during localization is very important. Generally, not until all particles' weights become zero and particle filter crash will we realize the localization has failed. However, the particle filter may have failed positioning correctly for a long time before we realize. Much noise may wipe out all the particles near the true state during the resampling phase. At the following resampling phases, the weights of some particles happen to be larger than zero. Then we have to run the particle filter longer to detect localization failure. In this period, the localization results may be arbitrary [24]. This is known as the kidnapped robot problem. In MaLoc, this problem may become more serious because we use a loose model instead of the Bayes filter model to evaluate the particles and the heuristic resampling method can increase the diversity, which cause the failure of particle filter need more time to expose.

In the experiments for analyzing the difference between the normal particle filter and "kidnapped" particle filter, we found that the clustering degree of particles reflects localization quality to some extent. In the initial phase, the particles are sampled from the initial area uniformly. After a series of steps, particles will tend to be centered around the true state in a small area. We name the size of this area as clustering degree. If both the motion model and measurement model are

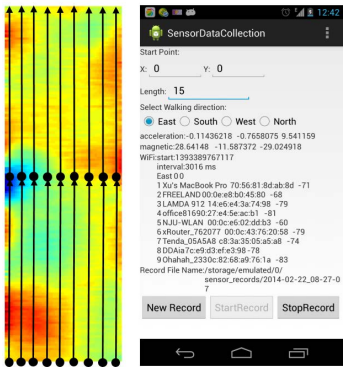

Figure 8. Fingerprints collection.

precise, the clustering degree will always keep very small. Errors in motion estimation or the measurement model may wipe out some particles closed to the true state and bring in some false-positive particles. These false-positive particles may converge to different directions. If the amount of false-positive particles is relative less, they will be wiped out in the following resampling phase very soon. Otherwise, it may need a long time or the amount of the false-positive particles is so large that they happen to wipe out all other true particles. However, in either case, they will result in enlarging clustering degree, especially the latter one. The enlargement phenomenon may disappear soon with more resampling. We hence use the clustering degree to predict the current localization error. Based on this localization error estimation method, we can heuristically detect the localization failure: if the predicted error $\hat{e}$ beyond a threshold T_{error}, the localization may has been failed. In MaLoc, the clustering degree is defined in the following way: the minimum radius r of a circle area which is centered around the current predicted location and the majority (i.e., 90%) of particles' positions are in this circle.

The localization data will be recorded in MaLoc, including the predicted result, the heading change $\Delta\theta$ and observation $\boldsymbol{z}$ in each step. When detecting localization failure, we can re-localize the user from a "stable" point. For example, from this point to the current point, there is no big heading change.

MAPPING THE MAGNETIC FIELD

There are many of magnetic mapping methods [17] or SLAM methods [26] proposed for robot localization based on magnetic field. In this section, we use crowdsourcing to enable fast and low-cost collection of the magnetic field fingerprints using smartphones. This method is inspired by IndoorAtlas [1]. As shown in Fig. 8, the data collector requires walking along these lines to cover an area. On each line, we set the starting point, the heading direction and the path length. We then walk along this path with a slow and constant speed. In this process, the tool application will record data captured by the magnetic sensor on smartphone. A magnetic fingerprint collected will be stored as $< B_h, B_v >$ and the magnitude can be computed from it. We simply assume the data collector walking at a constant speed. Each magnetic fingerprint can then be mapped with its location easily. To avoid large mapping errors, each line should not be too long. On each line, we collect intensive magnetic fingerprints, e.g., one fingerprint every 0.1 meter. The distance between the two lines is about 0.6 meter in our experiment. We then fill the fingerprints into this area by interpolation. Eventually, we obtain a magnetic fingerprint in every $0.1\text{m}\times0.1\text{m}$ square.

EXPERIMENTS

We now move to evaluate MaLoc. We conduct extensive experimental studies in a large building with a $72\text{m}\times64\text{m}$ floor plan, as shown in Fig. 9. The study involves 7 volunteers who are mainly students in a local university and several types of smartphones are used, including Samsung Galaxy, HTC, Moto. The MaLoc software is pre-installed into their smartphones for collecting user traces. We attach a stamper on the shoes of the volunteers. While he is walking, the stamper will put a stamp on the ground each step. By attaching permanent marks on the stamps, we can get all the experiments traces and their ground truth. For avoiding more tedious ground truth measurement, on the following trace collections, the volunteers are required to walk along these traces step by step. The total trace collections are conducted over a month. For experiments, we first focus on evaluating individual techniques we proposed: 1) How much step counting errors can MaLoc tolerate; 2) How well the dynamic step length estimation performs; 3) How well the heuristic resampling algorithm performs; 4) Performance comparison of particle filters with different types of magnetic fingerprinting models; 5) How accurate the localization quality estimation and localization failure detection algorithms achieve. We then evaluate the overall performance of MaLoc, including the overall localization accuracy under different conditions, the localization accuracy with different walking paths, and the energy consumption in comparison to the Wi-Fi fingerprinting based localization approach.

In the first experiment, we evaluate the influence of step counting error. Figure 10 shows both localization errors of the traditional particle filter and our augmented particle filter in presence of random miscounting steps. The user walks about 300 steps. The traditional particle filter functions correctly until miscounting reaches 50. However, our proposed particle filter tolerates more miscounting steps, i.e., 80 steps. It is not only because of the heuristic resampling method increases the diversity of particles, but also the dynamic step length estimation can compensate miscounting steps. In this experiment, the true step length of the user is about 0.6∼0.65m. The average estimated step length measured by our augmented particle filter is 0.68m when miscounting is 10 steps, but it increases to 0.77m when miscounting goes up to 50 steps.

Next, we test the particle filter with our proposed dynamic step length estimation. In this experiment, we set σ_l to 0.2 and Q_{size} to 5. The user's true step length is about 0.6∼0.65m. Figure 11 compares our augmented particle filter (without heuristic resampling) with the traditional one for localization errors when we set the step length to different values (i.e., 0.5m, 0.6m, 0.7m and 0.8m). As shown in the figure, when the step length deviates much from the true step length in the traditional particle filter, we observe poor accuracy. The tra-

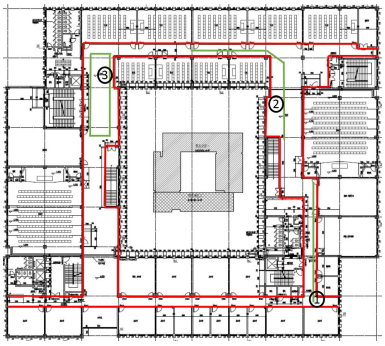

Figure 9. The floor map of the building.

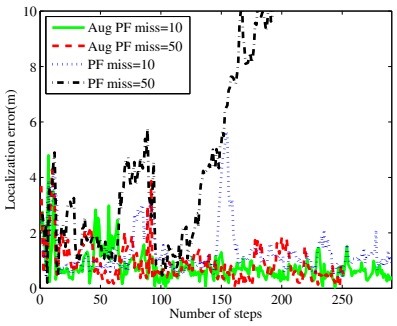

Figure 10. Localization results of two particle filters when miscounting occurred.

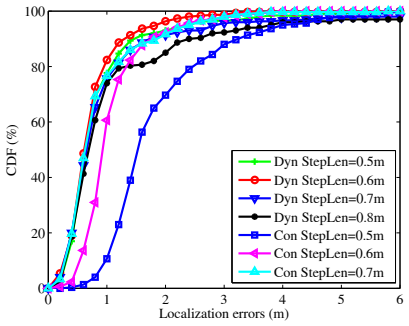

Figure 11. Performance of two particle filters with different initial step lengths.

ditional particle filter fails to localize when the step length is set to 0.8m. However, our augmented particle filter with dynamic step length estimation is not so sensitive to the initial step length. The experiments implies that although errors exist in the initial step length, the localization precision of our augmented particle filter is still quite good. In addition, we found that the average step length of the whole process of localization is around 0.7m, no matter what the initial step length is. This implies, after a period of time, we can infer the user's average step length. However, our dynamic step length estimation algorithm may fail when the initial step length deviates from the true step length too much. We hence set the average step length as the initial value in MaLoc, which works well in practise.

We now evaluate the heuristic resampling algorithm from two aspects: when processing the error of heading change estimation and when processing the occasional change of the heading offset. First, we run the particle filter 100 times with precise step counting and a constant step length, respectively. The traditional particle filter fails to localize 4 times as there are errors in heading change estimation causing localization failure. In contrast, our particle filter with the heuristic resampling algorithm localizes all correctly (i.e., 100 times), demonstrating more robust than the traditional particle filter. Second, we run an experiment to verify the ability of processing the occasional change of heading offset. We use a trace in which the user walks along a 24-meter corridor and answers a phone call while walking. We compare the traditional particle filter and our augmented particle filter for localizing his position. The results are presented in Fig. 12. We observe from the result that the heading offset change has only temporary influence on localization precision, but it causes the traditional particle filter converge to wrong locations.

To compare the performance of different types of magnetic observation values, we conduct an experiment in a hall, in which the traditional particle filter will need a longer period of time to converge. The user held his smartphone in hand and walked 69 steps in total. He started from a hall, walked about 27 steps and then turned left into a corridor. Figure 13 depicts the localization results of MaLoc using three different fingerprinting models as observation. As we observe from the figure, the HV fingerprint is sensitive to the user's turning motion but it has a faster convergence rate. Using the magnetic magnitude fingerprint is more robust, but it has a lower convergence rate than the HV fingerprint does. This shows clearly that the hybrid model certainly takes advantages of both models.

When we localize a trace, we will estimate the localization error using our localization quality estimation method and compare the predicted error with the true error. Among 42840 localization results, the average difference between the true error and the predicted error is about 0.96m. To evaluate the localization failure detection method, we analyze all the localization failure cases in out experiments. Out of 149 cases, 138 of them are detected by our failure detection method ($T_{error} = 7m$ in our experiment), resulting in an accuracy of 92.6%. In the 194 successful localization cases collected by us, the false positive rate is 8.2%. Figure 14 shows the true localization error and the predicted localization error of two experiments, respectively. Exp2 depicts success localization while Exp1 depicts localization failure.

In this experiment, we are interested to know how noise in motion estimation and the magnetic measurement affect localization accuracy and precision. We conduct five experiments with a user holding his smartphone with five different postures, including: 1) holding it by hand while keeping the same direction as his heading; 2) putting it in his shirt pocket; 3) putting in his pant pocket; 4) shaking it slightly left and right; 5) holding by hand and swinging along with his arm while walking. We then compare the localization results of MaLoc with the Wi-Fi fingerprinting based method, as shown in Fig. 15. The result shows that holding by hand yields the most accurate result because it has less noise in motion estimation and magnetic measurement. When putting the phone in pant pocket or shaking it while walking will result in decreasing of accuracy and precision. It implies that the more noise introduced during magnetic measurement and motion estimation, the greater decreased in localization accuracy. The average number of elements in each Wi-Fi fingerprint is 6.46 in our database, which is quite dense. The 50% and 80% errors of the Wi-Fi fingerprinting based approach are 2.5m and 4.5m, respectively, and the average localization accuracy is 3.5m. However, when holding the phone in hand, the results of MaLoc's 50% errors, 80% errors and the average accuracy are 0.7m, 1.8m, and 1m, respectively. Even in the worst case (i.e., putting the phone in the pant pocket), the

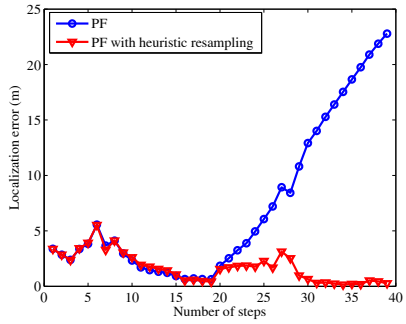

Figure 12. Localization results of two particle filters with heading offset change.

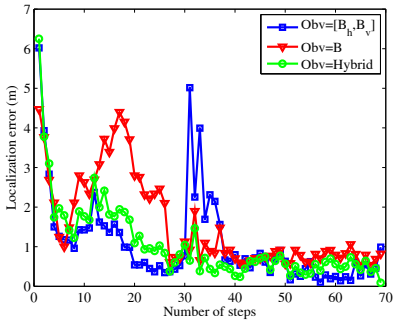

Figure 13. The performance of MaLoc using different types of observations.

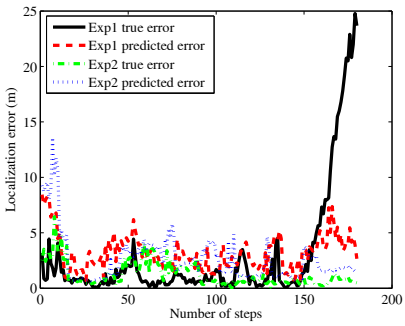

Figure 14. The true localization errors and predicted localization errors.

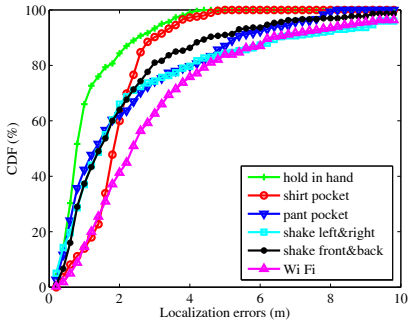

Figure 15. Performance of MaLoc in different conditions and performance comparison with Wi-Fi fingerprinting.

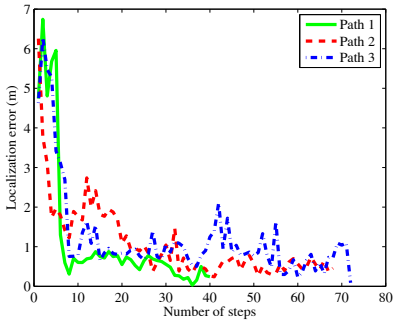

Figure 16. Performance of MaLoc in different trajectories.

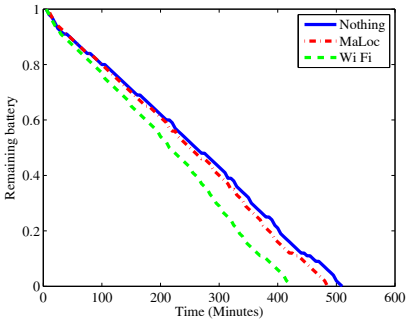

Figure 17. Energy efficiency of MaLoc, compared with Wi-Fi fingerprinting technology.

average localization accuracy of MaLoc is 2.8m which is also much better than Wi-Fi fingerprinting.

To evaluate the performance of MaLoc in different walking paths, we select three typical trajectories (as shown in Fig. 9): a straight line in corridor (Path 1), a trajectory with a corner in an open area (Path 2), and a rectangle trajectory in an open area (Path 3). Figure 16 depicts the localization results when a user walks along these trajectories. The result shows that converging in a corridor (i.e., Path 1) seems faster than the other two paths because of the physical limits of the map and any turning temporally decreases localization precision as new random particles are sampled.

In the last experiment, we evaluate the energy consumption of MaLoc. We conduct the experiments using a Samsung Galaxy Nexus smartphone, and compare the energy consumption in three scenarios: running nothing, running trace collection application of MaLoc only, and running the Wi-Fi scanning application only. All of the sensors' frequency in MaLoc are set to SENSOR_DELAY_NORMAL and the frequency of Wi-Fi scanning is set to 2 seconds. To prevent the smartphone from entering the hibernating mode and accelerate its energy consumption, we keep the smartphone's screen active during our experiment. Figure 17 shows the energy consuming of these three experiments. From the result, we observe that running MaLoc trace collection application saves about 1 hour battery life than running the Wi-Fi scanning application. The average current of the smartphone when running MaLoc is about 220mA. Thus, we conclude that MaLoc saves about 220mA·h energy than Wi-Fi scanning within about 6 hours.

CONCLUSION

In conclusion, this paper presents a novel indoor localization system named MaLoc. It utilizes magnetic sensor data and inertial sensor data on smartphones by an augmented particle filter. The most important feature of MaLoc is that it does not impose any restriction on smartphone's orientation, and users are free to use their phones in whatever ways they like during localization. We proposed a hybrid magnetic measurement model, which improves the performance of MaLoc and avoids calibrating different magnetometers. Moreover, we proposed a set of novel techniques to improve MaLoc's robustness and usability. Through comprehensive experiments based on the traces collected in a large building, we demonstrate that MaLoc is more accurate and energy efficient than the Wi-Fi fingerprinting based technique. However, the experimental study in this paper has a limited scope. We plan to further develop MaLoc and make it available for both Google Play and Apple Store, and collect public user traces in a variety of indoor spaces for more extensive evaluations.

ACKNOWLEDGMENTS

This work was supported by the NSFC under Grants 61373011, 91318301, the Foundation for Innovative Research Groups under Grant 61321491.

REFERENCES

1. https://www.indooratlas.com/.
2. Angermann, M., Frassl, M., Doniec, M., Julian, B. J., and Robertson, P. Characterization of the indoor magnetic field for applications in localization and mapping. In *IPIN*, IEEE (2012), 1–9.
3. Bahl, P., and Padmanabhan, V. N. Radar: An in-building rf-based user location and tracking system. In *INFOCOM*, vol. 2, IEEE (2000), 775–784.
4. Bilke, A., and Sieck, J. Using the magnetic field for indoor localisation on a mobile phone. In *Location-Based Services*. Springer, 2013, 195–208.
5. Chen, Y., Lymberopoulos, D., Liu, J., and Priyantha, B. Fm-based indoor localization. In *Mobisys*, ACM (2012), 169–182.
6. Chintalapudi, K., Padmanabha Iyer, A., and Padmanabhan, V. N. Indoor localization without the pain. In *Mobicom*, ACM (2010), 173–184.
7. Chung, J., and Donahoe. Indoor location sensing using geo-magnetism. In *Mobisys*, ACM (2011), 141–154.
8. Dellaert, F., Fox, D., Burgard, W., and Thrun, S. Monte carlo localization for mobile robots. In *Robotics and Automation*, vol. 2, IEEE (1999), 1322–1328.
9. Fox, D., Burgard, W., Dellaert, F., and Thrun, S. Monte carlo localization: Efficient position estimation for mobile robots. *AAAI/IAAI 1999* (1999), 343–349.
10. Hallberg, J., Nilsson, M., and Synnes, K. Positioning with bluetooth. In *ICT*, vol. 2, IEEE (2003), 954–958.
11. Haverinen, J., and Kemppainen, A. Global indoor self-localization based on the ambient magnetic field. *Robotics and Autonomous Systems 57*, 10 (2009), 1028–1035.
12. Le Grand, E., and Thrun, S. 3-axis magnetic field mapping and fusion for indoor localization. In *MFI*, IEEE (2012), 358–364.
13. Li, B., Gallagher, T., Dempster, A. G., and Rizos, C. How feasible is the use of magnetic field alone for indoor positioning? In *IPIN*, IEEE (2012), 1–9.
14. Li, F., Zhao, C., Ding, G., Gong, J., Liu, C., and Zhao, F. A reliable and accurate indoor localization method using phone inertial sensors. In *Ubicomp*, ACM (2012), 421–430.
15. Madigan, D., Einahrawy, E., Martin, R. P., Ju, W.-H., Krishnan, P., and Krishnakumar, A. Bayesian indoor positioning systems. In *INFOCOM*, vol. 2, IEEE (2005), 1217–1227.
16. Naqvi, N. Z., Kumar, A., Chauhan, A., and Sahni, K. Step counting using smartphone-based accelerometer. *International Journal on Computer Science & Engineering 4*, 5 (2012).
17. Navarro, D., and Benet, G. Magnetic map building for mobile robot localization purpose. In *ETFA*, IEEE (2009), 1–4.
18. Ozyagcilar, T. Calibrating an ecompass in the presence of hard and soft-iron interference. *Freescale Semiconductor Ltd* (2012).
19. Rai, A., Chintalapudi, K. K., and Padmanabhan. Zee: zero-effort crowdsourcing for indoor localization. In *Mobicom*, ACM (2012), 293–304.
20. Sen, S., Radunovic, B., Choudhury, R. R., and Minka, T. You are facing the mona lisa: spot localization using phy layer information. In *Mobisys*, ACM (2012), 183–196.
21. Storms, W., Shockley, J., and Raquet, J. Magnetic field navigation in an indoor environment. In *UPINLBS*, IEEE (2010), 1–10.
22. Subbu, K. P., Gozick, B., and Dantu, R. Locateme: Magnetic-fields-based indoor localization using smartphones. *TIST 4*, 4 (2013), 73.
23. Suksakulchai, S., Thongchai, S., Wilkes, D., and Kawamura, K. Mobile robot localization using an electronic compass for corridor environment. In *SMC*, vol. 5, IEEE (2000), 3354–3359.
24. Thrun, S., Burgard, W., and Fox, D. *Probabilistic robotics*. MIT press, 2005.
25. Thrun, S., Fox, D., Burgard, W., and Dellaert, F. Robust monte carlo localization for mobile robots. *Artificial intelligence 128*, 1 (2001), 99–141.
26. Vallivaara, I., Haverinen, J., Kemppainen, A., and Roning, J. Simultaneous localization and mapping using ambient magnetic field. In *MFI*, IEEE (2010), 14–19.
27. Varshavsky, A., de Lara, E., Hightower, J., LaMarca, A., and Otsason, V. Gsm indoor localization. *Pervasive and Mobile Computing 3*, 6 (2007), 698–720.
28. Want, R., Hopper, A., Falcao, V., and Gibbons, J. The active badge location system. *TOIS 10*, 1 (1992), 91–102.
29. Ward, A., Jones, A., and Hopper, A. A new location technique for the active office. *Personal Communications 4*, 5 (1997), 42–47.
30. Woodman, O., and Harle, R. Pedestrian localisation for indoor environments. In *Ubicomp*, ACM (2008), 114–123.
31. Youssef, M., and Agrawala, A. The horus wlan location determination system. In *Mobisys*, ACM (2005), 205–218.